J Mater Sci (2007) 42:2652–2661
DOI 10.1007/s10853-006-1358-z

Temperature and weldline effects on tensile properties of injection moulded short glass fibre PC/ABS polymer composite

S. Hashemi · Y. Lepessova

Received: 9 January 2006 / Accepted: 28 February 2006 / Published online: 4 January 2007

Abstract The effect of weldline and temperature on tensile properties of injection moulded PC/ABS blend reinforced with different concentration levels of short glass fibres was investigated between 23 and 100 °C. The weldline was formed in the moulded specimens by direct impingement of two opposing melt fronts. It was found that weldline had no significant effect on tensile modulus with weldline integrity factor in the range of 1–0.98. Tensile modulus for both weld and unweld specimens increased linearly with increasing volume fraction of fibres, φ_f, and decreased linearly with increasing temperature. Tensile strength of both weld and unweld tensile specimens increased non-linearly with increasing φ_f reaching a maximum at $\varphi_f \approx 0.16$ for specimens without weldline and $\varphi_f \approx 0.12$ for specimens with weldline. A linear dependence with respect to φ_f was found for both weld and unweld tensile strengths for fibre volume fractions in the range 0–0.1. It was found that below the glass transition temperature of the matrix, tensile strength of the composite with and without weldlines decreased linearly with increasing temperature. The weldline integrity factor for tensile strength decreased with increasing φ_f, but showed no significant variation with respect to temperature.

Introduction

It is well established that the mechanical properties of the polymer matrix (e.g. strength and modulus) are enhanced by the addition of short fibres [1–13]. These properties, however, are affected by a number of parameters, such as the concentration of the fibres, fibre length, fibre orientation and the degree of interfacial adhesion between the fibre and the matrix. However, as most short fibre composites are fabricated by an injection moulded process, a major design concern is the effect that weldlines may have on the mechanical properties of the polymer matrix and its composites. Weldlines are observed in injection moulded components due to multigate moulding, existence of pins, inserts, variable wall thickness and jetting and are classified as either being cold or hot. A cold weldline is formed when two melt fronts meet head on and this type of weldline is the worst-case scenario as far as mechanical properties are concerned. A serious reduction in strength has been reported for many polymers and their composites in the presence of cold weldlines [4–10]. However, very limited work has been done to investigate the effect of temperature on weldline strength. It is therefore desirable to determine to what extent temperature influences weldline properties. To this end, the present work was undertaken to examine the influence of temperature and weldline on tensile properties of PC/ABS blend reinforced with 5% to 50% by weight short glass fibres.

Experimental details

Materials

Owens Corning chopped E-glass fibres of approximately 4.0 mm in length and 10μm in diameter and a thermoplastic blend of polycarbonate (PC) and Acrylonitrile

S. Hashemi (✉) · Y. Lepessova
London Metropolitan Polymer Centre, London Metropolitan University, Holloway Road, London N7 8DB, UK
e-mail: s.hashemi@londonmet.ac.uk

Butadiene Styrene (ABS) as received by GE plastics (trade name Cycoloy C2800) were compounded in house to produce composites with nominal glass contents of 0, 5, 10, 20, 30, 50% w/w.

Compounding

The glass fibres and the pre-dried polymer pellets were dry blended to the desired glass content and compounded in a Brabender counter-rotating twin screw extruder with L/D ratio of 40:1 and a die of diameter 4 mm. The temperature profile along the extruder was 255/260/260 and the screw speed was 4–7 rpm. The extrudates were continuously cooled in a water bath and palletized and then dried in an oven at 90 °C for 3–4 h before being injection moulded into tensile bars.

Specimen preparation

Dumbbell shaped tensile bars of dimensions 1.7 mm × 12.5 mm × 125 mm as shown in Fig. 1 were produced on a Negri Bossi NB60 injection moulding machine using the processing conditions given in Table 1. The mould used consisted of a single- and a double-feed cavity details of which can be found in reference [5]. In the latter, the two opposing melt fronts met to form a weldline mid-way along the gauge length of the specimen.

Tensile tests

Dumbbell specimens with and without weldline were tested in tension at a crosshead speed of 50 mm/min in an Instron 4466 testing machine using pneumatic clamps. Tensile strength and modulus for both specimen types were measured at test temperatures of 23, 40, 60, 80 and 100 °C. For each material at least five specimens with weldline and five without weldline were tested at a given temperature. The load–displacement curve for each specimen was recorded using a computer data logger.

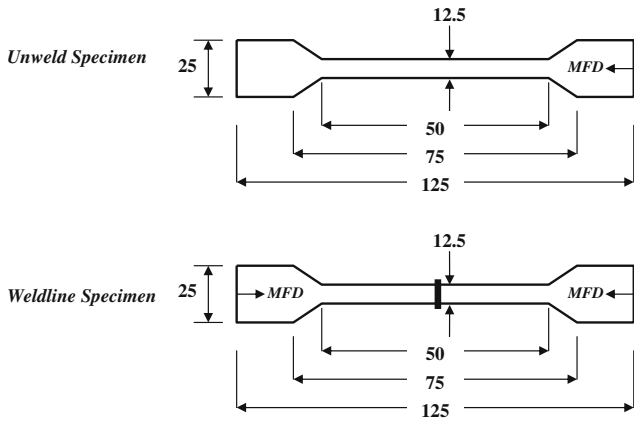

Fig. 1 Tensile specimens with and without weldline (all dimensions are in mm)

Table 1 Processing conditions

Processing parameters	
Melt temperature (°C)	250/255/260/265
Mould temperature (°C)	60
Cooling time (s)	25
Holding time (s)	3–5
Cycle time (s)	38–40
Holding pressure ($\times 10^5$ Pa)	15–20
Injection pressure ($\times 10^5$ Pa)	35–90

Measurement of fibre length and fibre concentration

Fibre concentration in each composite was determined from a weighed fibre samples removed from the gauge length of the moulded bars after ashing at 550 °C. After cooling, the ash of fibrous material was reweighed and the exact weight fraction of fibres, w_f was calculated. Since composite properties are linked to fibre volume fraction, φ_f, values of w_f were converted to φ_f using the following equation

$$\phi_f = \left[1 + \frac{\rho_f}{\rho_m}\left(\frac{1}{w_f} - 1\right)\right]^{-1} \quad (1)$$

Taking the density of the matrix, ρ_m as1.20 kg m^{-3} and that of the fibre, ρ_f as 2.54 kg m^{-3} gave φ_f values of 0.014, 0.045, 0.094, 0.161 and 0.287.

The residue from the ash tests were then spread on a glass slide and placed on the observation stage of a microscope. Magnified fibre images were transmitted to a large screen, and the fibre images were then automatically digitised by software with a computer and the fibre length distributions were thus determined from which the average fibre length, $\bar{L}_f$ in each composite was determined. As shown in Fig. 2, $\bar{L}_f$ decreased significantly with increasing φ_f thus indicating that the glass content played an important role in determining the average fibre length in injection moulded components. The increased damage to fibre length with φ_f was attributed to increased probability of fibre–fibre interaction at higher fibre loadings as well as an increased in melt viscosity resulting. The latter give rise to higher bending forces on the fibres during compounding and moulding process thus causing the fibres to break.

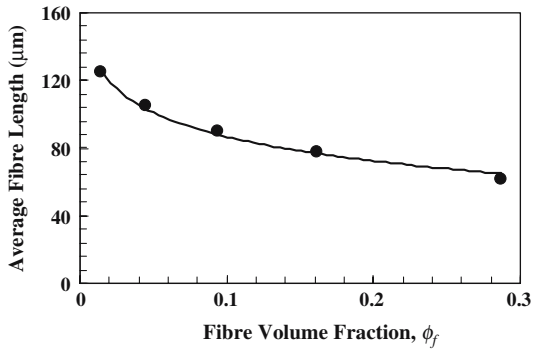

Fig. 2 Effect of fibre volume fraction on the average fibre length, $\bar{L}_f$

Results and discussions

Tensile modulus analysis

Fibre concentration effects

According to the load–displacement curves recorded for the non-weld specimens, deformation of the polymer blend acting as the matrix and its composites during the early stages of the deformation was linearly elastic. As expected, the addition of glass fibres to the polymer increased the initial slope of the load–displacement curves. Using the initial slope of the curves, the elastic modulus for specimens without weldline was calculated and plotted as a function of fibre volume fraction as shown in Fig. 3 for the temperature range of interest. It can be seen from the figure that tensile modulus increases linearly with increasing φ_f for the entire temperature range studied here. The simplest model that predicts a linear dependence between the composite modulus, E_c and the fibre volume fraction, φ_f is that of the modified

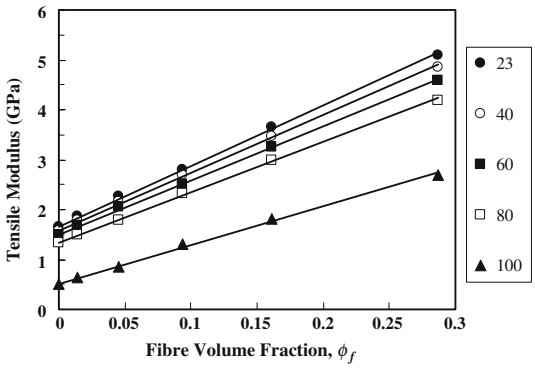

Fig. 3 Effect of fibre volume fraction on the tensile modulus in the absence of the weldline at 23, 40, 60, 80 and 100 °C

"rule-of-mixtures" equation. A simple rearrangement of the equation gives:

$$E_c = E_m + (\eta_E E_f - E_m)\phi_f \quad (2)$$

where E_m and E_f are the elastic moduli of the matrix and the fibre respectively and η_E is the fibre efficiency parameter for the composite modulus whose value depends on the length and the orientation of fibres in the moulded specimen. On the assumption that tensile modulus of the fibre, E_f is 76 GPa and not greatly influenced by the temperature, values of η_E as a function of temperature were calculated from the slope of the lines in Fig. 3 using Eq. 2. As shown in Fig. 4 fibre efficiency parameter η_E decreases with increasing temperature. A significant drop in η_E was obtained at glass transition temperature of the matrix ($T_g \approx 100$°C). As $\eta_E << 1$, it may be said that modulus of the composite specimens without weldline is significantly affected by the length and the orientation of the fibres in the moulded specimens.

The efficiency parameter η_E for the composite modulus is defined as

$$\eta_E = \eta_L \eta_o \quad (3)$$

where η_L and η_o are the fibre length and orientation efficiency parameters, respectively. Note that $\eta_o = 1$ for aligned-longitudinal orientation, $\eta_o = 0$ for aligned-transverse orientation and $\eta_o = 0.375$ for random in-plane orientation of fibres.

The η_L for all five composites as a function of temperature was computed from the average fibre lengths in Fig. 2 using the Cox shear lag model [14] which defines η_L as:

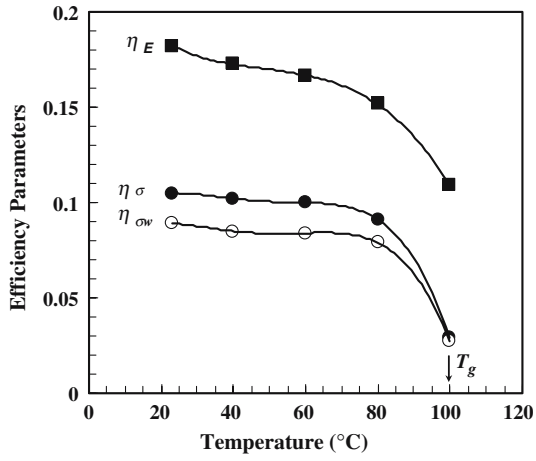

Fig. 4 Effect of temperature on fibre efficiency parameters for composite modulus and strength for specimens with and without weldlines

$$\eta_L = 1 - \frac{\tanh \beta}{\beta} \tag{4}$$

with

$$\beta = \frac{\bar{L}_f}{2}\left(\frac{4E_m}{E_f d^2 \ln \lambda}\right)^{\frac{1}{2}} \tag{5}$$

where d is the diameter of the fibres. For an assumed square packing arrangement of fibres λ is

$$\lambda = \sqrt{\frac{\pi}{4\phi_f}} \tag{6}$$

The values of η_L calculated using Eq. 4 and the corresponding values of η_o calculated using Eq. 3 are tabulated in Table 2. It can be seen that whilst η_L does not vary significantly with φ_f it decreases with increasing temperature with a significant drop in value occurring at T_g. As for η_o, it can be seen from Table 2 that this parameter shows no significant variation with respect to φ_f and below the T_g it is also unaffected by the temperature having an average value of 0.648. At T_g the average value for η_o rises rapidly to 0.987. We can only assume that due to viscous nature of the polymer matrix at T_g fibres are able to rotate towards the direction that the matrix material is being stressed.

Using the Krenchel [15] definition of η_o

$$\eta_o = \sum_{i=1}^{i=n} a_n \cos^4 \theta_n \tag{7}$$

and assuming a perfect alignment of fibres (i.e. $a_n = 1$), we estimate that η_o of 0.648 corresponds to a fibre orientation angle, θ of approximately 26° and η_o of 0.987 corresponds to a fibre orientation angle of approximately 5°.

Temperature effects

The modulus of the matrix and its composites decreased with increasing temperature and dropped significantly at T_g. However, as shown in Fig. 5, below the T_g modulus of the non-weld specimens decreases linearly with increasing temperature at a rate which is dependent upon the volume fraction of fibres in the composite. Evidently, the decrease occurs at a faster rate when φ_f is high. According to the data in Fig. 5, the linear dependence between modulus and temperature for non-weld specimens can be expressed as

$$E(T) = E_0 - \kappa T \tag{8}$$

where E_0 and κ are constants whose values at a given temperature increased with increasing φ_f.

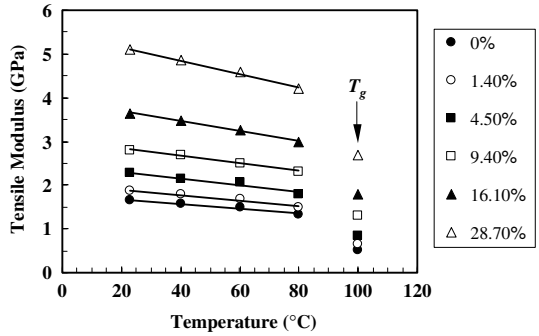

Fig. 5 Effect of temperature on the tensile modulus in the absence of the weldline at various fibre concentration levels (%v/v)

Weldline effects

As regards weldline and its influence on tensile modulus, it was noted that the deformation of the matrix and its composites in the ''elastic region'' was only marginally affected by the presence of the weldline. The modulus retention ratio or the weldline integrity parameter as it is commonly known (the ratio of the modulus of a specimen with a weldline to that of a specimen without a weldline) ranged between 1.0 and 0.98 and showed no systematic variation with respect to either temperature or fibre volume fraction. The weldline integrity factors of near unity suggest that the presence of weldline had little effect, if any, on tensile modulus. This behaviour was interpreted using

Table 2 Fibre efficiency parameters for composite modulus as a function of fibre volume fraction at 23, 40, 60, 80 and 100 °C

φ_f	η_E					η_L					η_o				
	23	40	60	80	100	23	40	60	80	100	23	40	60	80	100
0.014	.182	.173	.166	.152	.109	.278	.270	.259	.238	.111	.655	.641	.640	.638	.978
0.045	.182	.173	.166	.152	.109	.277	.269	.258	.237	.111	.657	.644	.643	.641	.984
0.094	.182	.173	.166	.152	.109	.275	.267	.256	.235	.110	.662	.648	.648	.646	.993
0.161	.182	.173	.166	.152	.109	.276	.268	.257	.236	.110	.659	.645	.645	.643	.987
0.0287	.182	.173	.166	.152	.109	.275	.267	.256	.235	.110	.662	.648	.647	.646	.992

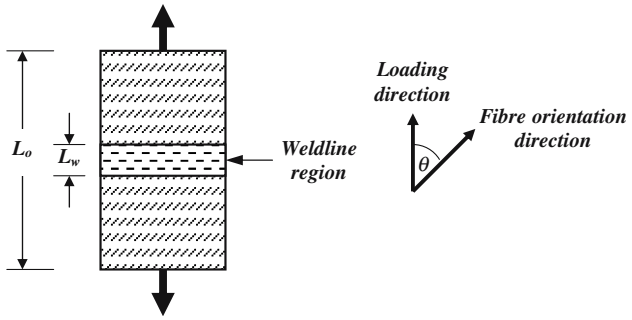

Fig. 6 Model for the prediction of the tensile modulus in the presence of a weldline

the model shown in Fig. 6 where E_{cw} represents modulus of the specimen with weldline, E_w modulus of the material inside the weldline and E_c modulus of the material outside the weldline. The optical light micrographs of the weld and unweld regions revealed that whilst fibres inside the weldline region were predominantly aligned with their long axis parallel to the weldline (i.e. perpendicular to the mould-fill direction and the direction of the applied tensile stress), outside the weldline region fibres were predominantly aligned in the same direction as in non-weld specimens (a fibre orientation angle of approximately 26°). The off-axis alignment of fibres outside the weldline region and the transverse alignment of fibres inside the weldline region, implies that $E_c >> E_w$. Assuming linear elastic deformation and considering that the total extension of the weld specimen is the sum of the extensions produced by its weld and unweld regions, gives the following relationship for E_{cw}:

$$\frac{1}{E_{cw}} = \frac{1-z}{E_c} + \frac{z}{E_w} \tag{9}$$

where $z = L_w/L_o$. Rearranging Eq. 9 gives the following relationship for E_{cw}

$$E_{cw} = \frac{E_c E_w}{E_w - (E_w - E_c)z} \tag{10}$$

Since the width of the weldline region, L_w was typically less than 1 mm and therefore much smaller than the overall length of the specimen (L_o), ratio z becomes very small and therefore the second term in denominator of Eq. 10 becomes small compared to E_w, thus indicating that $E_{cw} \approx E_c$, i.e., weldline has little effect on tensile modulus as observed in this study.

It is worth stating, that below the T_g, modulus of the weldline specimens like non-weld specimens decreased linearly with increasing temperature and followed Eq. 7 with almost the same values of E_0 and κ as used to describe modulus-temperature data of the non-weld specimens.

Tensile strength analysis

Fibre concentration effects

The effect of fibre volume fraction on tensile strength of the specimens without weldline at various temperatures is shown in Fig. 7 (The value at $\varphi_f = 0$ represents the tensile strength of the unfilled matrix). Evidently, in the absence of weldline, tensile strength increases with increasing fibre concentration and reaches a maximum at $\varphi_{max} \approx 0.16$ before decreasing with further addition of short fibres. This negative reinforcement effect beyond $\varphi_{max} \approx 0.16$ has also been noted in other injection moulded glass reinforced polymer systems such as polypropylene, nylon6,6, polybutylene terephthalate and styrene maleic anhydride [10–13]. The negative effect is mainly attributed to the separation distance between the fibres becoming sufficiently small beyond $\varphi_{max} \approx 0.16$ that the flow of the matrix material between fibres is severely restricted. This effect and the higher stress concentration in the matrix due to the greater number of fibre ends at high φ_f, could reduce the gain in strength which one would expect otherwise.

The non-linear relationship in Fig. 7 between the tensile strength of the composite specimens without weldline, σ_c and the fibre volume fraction, φ_f can be described by a polynomial function of the form:

$$\sigma_c = a_0 + a_1\phi_f + a_2\phi_f^2 \tag{11}$$

where a_0, a_1 and a_2 are the curve fitting parameters whose values vary with temperature as illustrated in Fig. 8. These curve fitting parameters can be used to predict the tensile strength of PC/ABS composites for

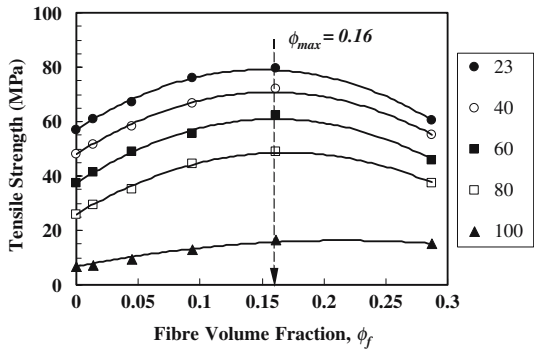

Fig. 7 Effect of fibre volume fraction on tensile strength in the absence of the weldline at 23, 40, 60, 80 and 100 °C

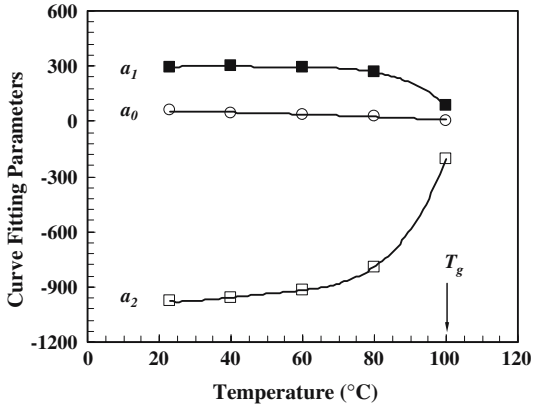

Fig. 8 Effect of temperature on curve fitting parameters of Eq. 11

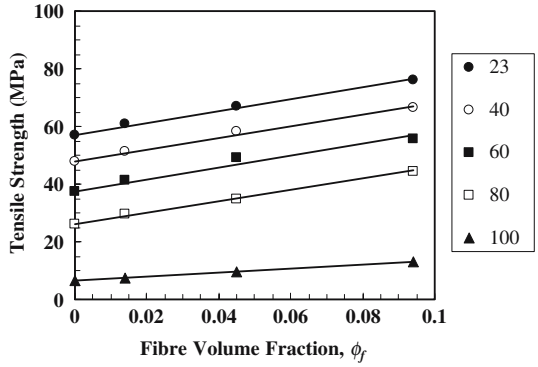

Fig. 9 Effect of fibre volume fraction on the tensile strength in the absence of weldline at various temperatures for fibre volume fractions less than φ_{max}

any combination of φ_f and T. It must be said however, that as far as composite strength is concerned, it is not advantageous to have fibre loadings exceeding 16%v/v since above this value, tensile strength in the absence of weldline decreased rather than increase. However, as shown in Fig. 9, below $\varphi_{max} \approx 0.16$, tensile strength increases linearly with φ_f. The simplest equation that predicts a linear dependence between σ_c and φ_f for short fibre composites is that of the modified rule-of-mixtures equation:

$$\sigma_c = \sigma_m + (\eta_\sigma \sigma_f - \sigma_m)\phi_f \quad (12)$$

where η_σ is the fibre efficiency parameter for the composite strength taking into account the effects due to fibre length and orientation in the composite, σ_f is the tensile strength of the fibre and σ_m is the tensile strength of the matrix. The intercept values at $\varphi_f = 0$, obtained from the best linear regression lines in Fig. 9 are within 1–2% of the matrix tensile strength with regression coefficients in the range 0.960–0.997.

Using Eq. 12 values of η_σ were calculated from the slope of the lines in Fig. 9 taking σ_f as 2,470 MPa. It can be seen from Fig. 4 that η_σ is considerably smaller than η_E and like η_E it decreases with increasing temperature. The efficiency parameter η_σ like η_E is defined as:

$$\eta_\sigma = \eta_L \eta_o \quad (13)$$

where η_L is the fibre length and η_o is the fibre orientation efficiency parameters for the composite strength. Using the η_o values obtained via the modulus data (see Table 2), η_L for composite strength was evaluated as a function of temperature using Eq. 13. It can be seen from Table 3 that η_L for composite strength like for composite modulus decreases with increasing temperature. However, η_L for strength is considerably smaller and is more sensitive to φ_f than η_L for modulus, thus explaining why η_σ is smaller than η_E.

Using the tabulated values of η_L in Table 3 and the average fibre length, $\bar{L}_f$ values in Fig. 2, the critical fibre lengths, L_c was calculated for each composite as a function of temperature using the Kelly–Tyson relationship [1]:

$$L_c = \frac{\bar{L}_f}{2\eta_L} \quad (14)$$

Results obtained from this analysis are presented in Table 4 where it can be seen that L_c increases with temperature but decreases with increasing φ_f mainly due to the reduction in $\bar{L}_f$ with increasing φ_f.

Temperature effects

The effect of temperature on the tensile strength of the specimens without weldline is shown more explicitly in

Table 3 Fibre efficiency parameters for composite strength as a function of fibre volume fraction at 23, 40, 60, 80 and 100 °C

φ_f	η_σ					η_o					η_L				
	23	40	60	80	100	23	40	60	80	100	23	40	60	80	100
0.014	.105	.102	.100	.091	.029	.648	.652	.646	.637	.951	.162	.156	.155	.143	.0305
0.045	.105	.102	.100	.091	.029	.650	.655	.649	.640	.957	.162	.156	.154	.142	.0303
0.094	.105	.102	.100	.091	.029	.655	.659	.653	.645	.965	.160	.155	.153	.141	.0301

Table 4 Fibre critical length as a function of fibre volume fraction at 23, 40, 60, 80 and 100 °C

φ_f	η_L					$L_c(\mu m)$				
	23	40	60	80	100	23	40	60	80	100
0.014	.160	.159	.156	.143	.0297	390	393	400	438	2,108
0.045	.160	.158	.156	.142	.0295	329	331	338	370	1,781
0.094	.159	.157	.154	.141	.0292	283	285	292	319	1,541

Fig. 10 where it can be seen that below T_g tensile strength decreases with temperature in a linear manner. Evidently, slope of the lines for values of φ_f in the range 0–0.16 is not affected significantly by the volume fraction of fibres and therefore within this range the effect of increasing φ_f is simply an upward vertical shift in tensile strength–temperature curve.

The linear dependence between tensile strength and temperature for φ_f values in the range 0–0.16 can be reasonably expressed by the following relationship;

$$\sigma(T) = \sigma_0 - 0.54\,T \tag{15}$$

where σ_o depends on φ_f and increases with increasing φ_f.

Weldline effects

Specimens with weldline always failed at the weldline region. Figure 11 shows tensile strength of the specimens with weldline, σ_{cw} as a function of fibre volume fraction, φ_f at various temperatures. It can be seen that σ_{cw} like σ_c increases with increasing φ_f in a non-linear manner. The maximum in σ_{cw} occurs at $\varphi_{max} \approx 0.12$ compared to 0.16 for σ_c. As illustrated in Fig. 11, variation of σ_{cw} with φ_f like σ_c can be expressed as

$$\sigma_{cw} = a_0 + a_1\,\phi_f + a_2\,\phi_f^2 \tag{16}$$

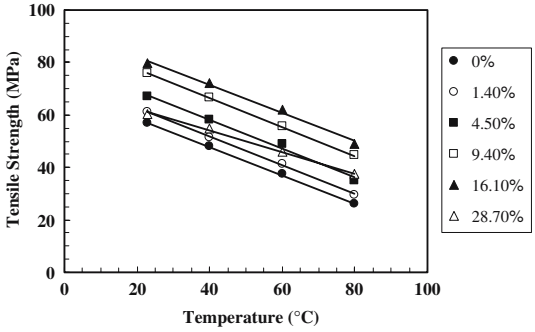

Fig. 10 Effect of temperature on the tensile strength in the absence of weldline at various fibre concentration levels (%v/v) for ($T < T_g$)

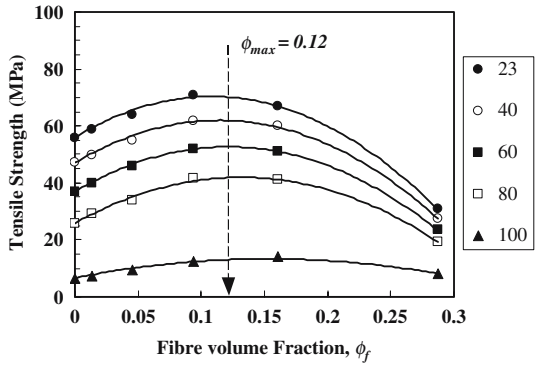

Fig. 11 Effect of fibre volume fraction on tensile strength in the presence of a weldline at 23, 40, 60, 80 and 100 °C

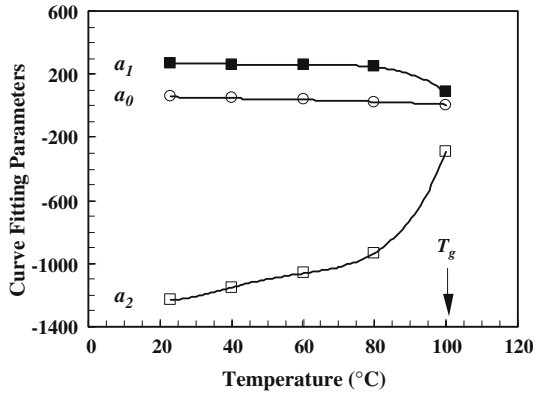

Fig. 12 Effect of temperature on curve fitting parameters of Eq. 16

Values of curve fitting parameters a_0, a_1 and a_2 as a function of temperature are shown in Fig. 12 where it can be seen that variation is similar to that obtained from specimens without weldline (see Fig. 8). However as illustrated in Fig. 13, the relationship between σ_{cw} and φ_f is remarkably linear for fibre volume fractions of less than 0.12. In fact the φ_f range for which both strengths tends to be linearly dependent upon φ_f is 0–0.10. Consequently, as for σ_c the linear dependence between σ_{cw} and φ_f was described using the modified rule-of- mixtures equation:

$$\sigma_{cw} = \sigma_{mw} + (\eta_{\sigma w}\sigma_f - \sigma_{mw})\phi_f \tag{17}$$

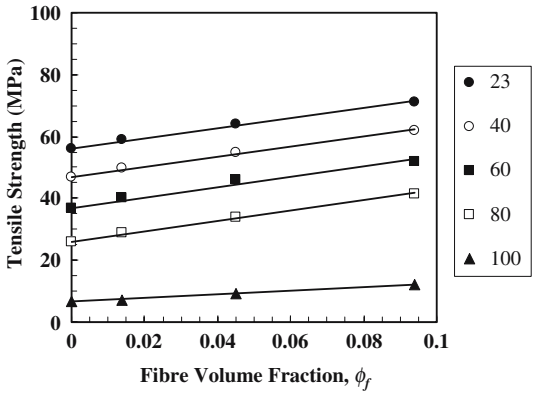

Fig. 13 Effect of fibre volume fraction on tensile in the presence of a weldline at various temperatures for fibre volume fractions less than φ_{max}

where σ_{mw} is the tensile strength of the matrix and $\eta_{\sigma w}$ is the fibre efficiency parameter for the composite strength, in the presence of weldline. Using Eq. 17 values of $\eta_{\sigma w}$ as a function of temperature were calculated from slope of the lines in Fig. 13. It can be seen from Fig. 4 that $\eta_{\sigma w}$ is smaller than η_σ but like η_σ it decreases with increasing temperature. It is worth noting that $\eta_{\sigma w} \approx \eta_\sigma$ at the glass transition temperature thus indicating that at this temperature weldline had no significant effect upon fibre efficiency parameter.

The effect of temperature on σ_{cw} is shown more explicitly in Fig. 14. It can be seen that below T_g the value of σ_{cw} like σ_c decreases linearly with increasing temperature. It is also evident that the slope of the lines for φ_f values in the range 0–0.10 is not affected significantly by the volume fraction of fibres and therefore within this range the effect of increasing φ_f is simply an upward vertical shift in weldline strength–temperature curve, as it was for σ_c.

The linear dependence between σ_{cw} and temperature for φ_f values in the range 0–0.1 can be reasonably expressed by the following relationship;

$$\sigma(T) = \sigma_0 - 0.52T \tag{18}$$

where σ_o depends on φ_f and increases with increasing φ_f.

The effect of weldline on tensile strength can be quantitatively expressed in terms of weldline integrity factor, F_σ defined as:

$$F_\sigma = \frac{\text{Tensile strength of specimen with weldline}}{\text{Tensile strength of specimen without weldline}} \tag{18}$$

Figure 15 shows the variation of F_σ with φ_f over the temperature range of interest. It is seen that F_σ decreases with increasing φ_f and shows very little variation, if any, with respect to temperature. The observed reduction in tensile strength in the presence of weldline is attributed mainly to the reduction in the fraction of fibres crossing the weldline region, particularly at high concentration values of glass fibres. As a result, the material within the weldline region acted as if it was not reinforced. As depicted in Fig. 16 when values of F_σ are plot against φ_f^2 a linear dependence is obtained which may be expressed as

$$F_{c\sigma} = F_{m\sigma}\left(1 - \gamma\phi_f^2\right) \tag{19}$$

where $F_c\sigma$ is the weldline integrity factor for composite strength, $F_m\sigma$ is the weldline integrity factor for the matrix strength and $\gamma = 5.37$. The regression coefficient for the line is 0.996.

Tensile strength versus modulus

The results concerning the effect of temperature on tensile strength and modulus were analysed further using the general form of the relationship between shear stress, τ and shear modulus, G as proposed by

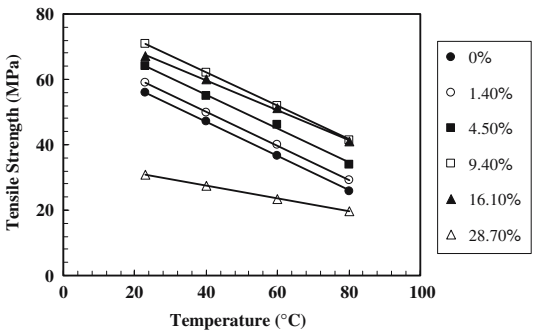

Fig. 14 Effect of temperature on strength in the presence of a weldline at various fibre concentration levels (%v/v) for ($T < T_g$)

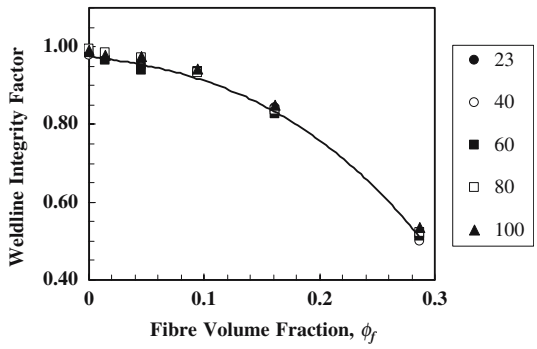

Fig. 15 Weldline integrity factor for tensile strength versus fibre concentration at 23, 40, 60, 80 and 100 °C

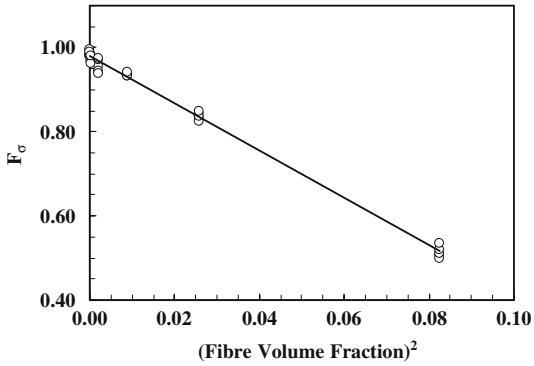

Fig. 16 Weldline integrity factor for tensile strength versus fibre volume fraction squared, φ_f^2 at various temperatures

Kitagawa [16]. This relationship is represented by a power law relation of the form:

$$\frac{T_0\tau}{T\tau_0} = \left(\frac{T_0 G}{T G_0}\right)^n \tag{20}$$

where τ_0 and G_0 are the values of shear stress and shear modulus at some reference temperature T_0, respectively and n is a temperature independent exponent. The shear properties (G,τ) in Eq. 21 were converted into tensile properties (E, σ) using the following relationship

$$\frac{\tau}{\tau_0} = \frac{\sigma}{\sigma_0} = \frac{E}{E_0} = \frac{G}{G_0} \tag{21}$$

Substituting Eq. 22 into Eq. 21 and rearranging gives

$$\ln\left(\frac{\sigma}{T}\right) = \ln\left[\left(\frac{T_0}{E_0}\right)^n \left(\frac{\sigma_0}{T_0}\right)\right] + n\ln\left(\frac{E}{T}\right) \tag{22}$$

According to Eq. 22 log–log plot of (σ/T) versus (E/T) should produce a straight line with the slope of n. Figures 17 and 18 show log–log plots according to

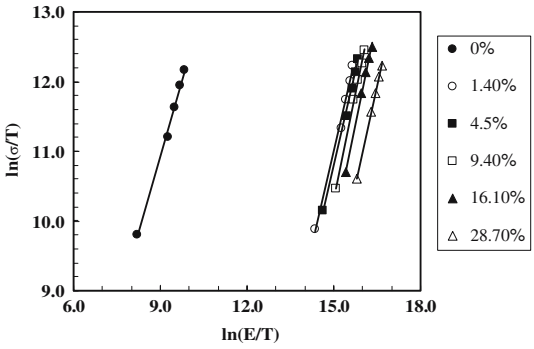

Fig. 17 $\ln(\sigma/T)$ versus $\ln(E/T)$ according to Eq. 22 for specimens without weldline at various fibre concentration levels (temperature T is in °K)

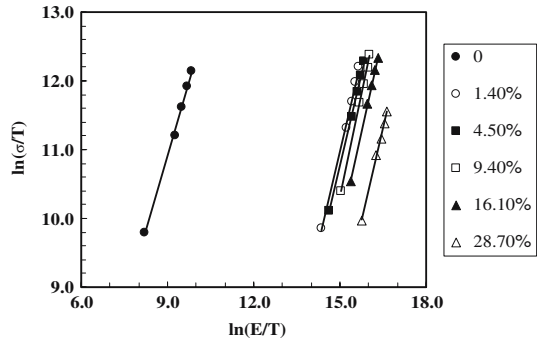

Fig. 18 $\ln(\sigma/T)$ versus $\ln(E/T)$ according to Eq. 22 for specimens with weldline at various fibre concentration levels (temperature T is in °K)

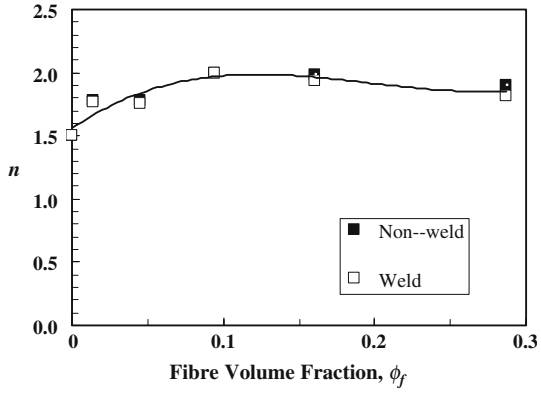

Fig. 19 The exponent n versus fibre volume fraction for weld and unweld tensile specimens

Eq. 22 for both unweld and weld strengths respectively for the range of φ_f values studied in this work. It is found that weld and unweld tensile strengths for the matrix and its composites follow Eq. 23 remarkably well with regression coefficients of 0.996 or better. The values of n obtained from the slope of the lines are plotted in Fig. 19 as a function of φ_f. It can be seen that although n is affected by the volume fraction of fibres it is not affected by the specimen type. According to Fig. 19, the exponent n increases with increasing φ_f and reaches a maximum value at $\varphi_f \approx 0.16$.

Conclusions

In this work the effect of temperature and weldline on tensile strength and modulus of PC/ABS blend reinforced with different concentration levels of short glass fibres was investigated between 23 and 100 °C. The following conclusions are obtained from the analysis of tensile test results.

- Tensile modulus increased linearly with increasing volume fraction of glass fibres, φ_f. The linear dependence between tensile modulus and φ_f obeyed the modified rule of mixtures for modulus.
- Tensile modulus decreased with increasing temperature. Below the glass transition temperature, modulus of the matrix and its composites decreased linearly with increasing temperature.
- Weldline had no significant effect on tensile modulus. Weldline integrity factor for modulus was in the range 0.98–1.0.
- Tensile strength of the specimens with and without weldline increased with increasing φ_f in a non-linear manner reaching a maximum for both specimen types before decreasing thereafter. The maximum tensile strength for specimens without weldline was observed at $\varphi_f \approx 0.16$ and for specimens with weldline at $\varphi_f \approx 0.12$. These φ_f values were not affected by the temperature.
- For fibre concentration values in the range 0–10%, the dependence of weld and unweld tensile strengths on φ_f was reasonably linear and obeyed the modified rule of mixtures for strengths.
- Weld and unweld tensile strengths decreased with increasing temperature. Below the glass transition temperature variation was reasonably linear for both specimen types.
- The fibre efficiency parameters for composite strength and modulus decreased with increasing temperature. The efficiency parameter for unweld tensile strength was greater than for weldline strength and both were considerably smaller than the fibre efficiency parameter for composite modulus.
- Weldline integrity factor for tensile strength decreased with increasing φ_f but showed no significant variation with respect to temperature. A linear dependence was obtained between weldline integrity factor and φ_f^2.

References

1. Kelly A, Tyson WR (1965) J Mech Phys Solids 6:13
2. Piggott MR, Ko M, Chuang HY (1993) Compos Sci Technol 48:291
3. Piggott MR (1994) J Compos Mater 28:588
4. Hashemi S, Gilbride MT, Hodgkinson JM (1996) J Mater Sci 31:5017
5. Din KJ, Hashemi S (1997) J Mater Sci 32:375
6. Chrysostomou A, Hashemi S (1998) J Mater Sci 33:1165
7. Nabi ZU, Hashemi S (1998) J Mater Sci 33:2985
8. Chrysostomou A, Hashemi S (1998) J Mater Sci 33:4491
9. Fu S-Y, Lauke B, Mader E, Yue C-Y, Hu X (2000) . Compos Part A 31:1117
10. Hashemi S (2002) Plast, Rubber Compos 31:318
11. Thomason JL (2002) Compos Sci Technol 62:1455
12. Thomason JL (2001) Compos Sci Technol 61:2007
13. Thomason JL (2002) Compos Part A. 33:331
14. Cox HL (1952) Br J Appl Phys 3:72
15. Krenchel H (1964) Fiber reinforcement. Akad Forlag, Copenhagen
16. Kitagawa M (1977) J Polym Sci 15:1601